[Channels 1:3, 144-147; May/June 2007]; ©2007 Landes Bioscience

Addendum

Mutation Associated with an Autosomal Dominant Cone-Rod Dystrophy CORD7 Modifies RIM1-Mediated Modulation of Voltage-Dependent Ca^{2+} Channels

Takafumi Miki[1]
Shigeki Kiyonaka[1]
Yoshitsugu Uriu[1]
Michel De Waard[2]
Minoru Wakamori[1,3]
Aaron M. Beedle[4]
Kevin P. Campbell[4]
Yasuo Mori[1,*]

[1]Department of Synthetic Chemistry and Biological Chemistry; Graduate School of Engineering; Kyoto University; Kyoto, Japan

[2]Inserm U607; Laboratorie Canaux Calciques; Fonctions et Pathologies; Grenoble Cedex, France

[3]Department of Oral Biology; Graduate School of Dentistry; Tohoku University; Sendai, Japan

[4]Howard Hughes Medical Institute and Department of Molecular Physiology and Biophysics; Internal Medicine and Neurology; University of Iowa Roy J. and Lucille A. Carver College of Medicine; Iowa City, Iowa USA

*Correspondence to: Yasuo Mori; Department of Synthetic Chemistry and Biological Chemistry; Graduate School of Engineering; Kyoto University; Kyoto 615-8510 Japan; Tel.: 81.75.383.2761, Fax: 81.75.383.2765; Email: mori@sbchem.kyoto-u.ac.jp

Original manuscript submitted: 06/28/07
Manuscript accepted: 06/29/07

This manuscript was previously published online as a *Channels* E-publication.

KEY WORDS

$Ca_v2.1$ channels, $Ca_v1.4$ channels, cone-rod dystrophy, RIM1, modulation, presynapse, whole-cell recording

ACKNOWLEDGEMENTS

See page 146.

Addendum to:

RIM1 Confers Sustained Activity and Neurotransmitter Vesicle Anchoring to Presynaptic Ca^{2+} Channels

S. Kiyonaka, M. Wakamori, T. Miki, Y. Uriu, M. Nonaka, H. Bito, A.M. Beedle, E. Mori, Y. Hara, M. De Waard, M. Kanagawa, M. Itakura, M. Takahashi, K.P. Campbell and Y. Mori

Nat Neurosci 2007; 10:691-701

ABSTRACT

Genetic analyses have revealed an association between the gene encoding the Rab3A-interacting molecule (RIM1) and the autosomal dominant cone-rod dystrophy CORD7. However, the pathogenesis of CORD7 remains unclear. We recently revealed that RIM1 regulates voltage-dependent Ca^{2+} channel (VDCC) currents and anchors neurotransmitter-containing vesicles to VDCCs, thereby controlling neurotransmitter release. We demonstrate here that the mouse RIM1 arginine-to-histidine substitution (R655H), which corresponds to the human CORD7 mutation, modifies RIM1 function in regulating VDCC currents elicited by the P/Q-type $Ca_v2.1$ and L-type $Ca_v1.4$ channels. Thus, our data can raise an interesting possibility that CORD7 phenotypes including retinal deficits and enhanced cognition are at least partly due to altered regulation of presynaptic VDCC currents.

Originally identified as a putative effector for the synaptic vesicle protein Rab3, RIM1 is expressed in the brain and retinal photoreceptors where it is localized to presynaptic ribbons in ribbon synapses.[1] RIM1 interacts with other presynaptic active-zone protein components, including Munc13, ELKS (also known as CAST), RIM-BP and liprins, to form a protein scaffold in the presynaptic nerve terminal.[2-6] Mouse knockout studies revealed that, in different types of synapses, RIM1 is essential for Ca^{2+}-triggered neurotransmitter release as well as different forms of synaptic plasticity.[5,7,8]

A mutation has been identified for an autosomal dominant cone-rod dystrophy CORD7 in the *RIM1* gene that is localized to chromosome 6q14.[9] A four-generation British family with CORD7 first experienced reduced color vision and visual acuity between the ages of 20 and 40 years. As the disorder progressed, they had difficulty seeing in bright light, and one individual reported visual problems in dim light. At the onset of symptoms, retinal pigmentary changes were already present around the fovea, simulating bull's eye dystrophy, which developed into macular atrophy.[10] Interestingly, the affected individuals also showed significantly enhanced cognitive abilities across a range of domains.[11] Thus, the CORD7 RIM1 mutation is characterized by retinal dystrophy and enhanced brain function. However, the mechanisms underlying these phenotypes are yet to be elucidated.

We recently revealed a previously unknown interaction between two components of the presynaptic active zone, RIM1 and VDCCs,[12] that is essential for Ca^{2+}-triggered neurotransmitter release.[13] RIM1 associates with VDCC β-subunits via the C terminus to markedly suppress voltage-dependent inactivation among different neuronal VDCCs. In addition, membrane docking of vesicles is also enhanced by RIM1. In pheochromocytoma neuroendocrine PC12 cells and in cultured cerebellar neurons, neurotransmitter release is significantly potentiated by RIM1. Thus, RIM1 association with VDCC β in the presynaptic active zone supports release via two mechanisms: sustaining Ca^{2+} influx through inhibition of channel inactivation, and anchoring neurotransmitter-containing vesicles in the vicinity of VDCCs. Here, we specifically test whether the RIM1 mutation associated with CORD7 affects RIM1 regulation of VDCC current inactivation in order to gain insight into the molecular mechanisms that underlying the two observed phenotypes in CORD7 patients.

A nucleotide (G to A) substitution, that replaces Arg-655 with His in the middle C_2A domain (Fig. 1A) reported for its ability to bind to VDCC α_1-subunit,[6] was introduced in the mouse RIM1 cDNA to yield a construct which carries a mutation corresponding to human CORD7 RIM1 mutation R844H.[9] The mouse clone differs from the human clone in having a deletion in the region between the Zn^{2+}-finger-like and PDZ domains. In this region, no specific functional domains have yet been identified. Co-immunoprecipitation experiments suggested an intact interaction between RIM1 mutant R655H and the VDCC β_{4b}-subunit (Fig. 1B). To elucidate the functional effects of the RIM1 mutant, we characterized whole-cell Ba^{2+} currents through recombinant VDCCs expressed as $\alpha_1\alpha_2/\delta\beta_{4b}$ complexes containing neuronal α_1-subunits $Ca_v2.1$ of P/Q-type VDCCs or $Ca_v1.4$ of L-type VDCCs. These VDCCs were selected, because P/Q-type $Ca_v2.1$ plays an important role in neurotransmitter release from central neurons,[13] while L-type $Ca_v1.4$ is found at high densities in photoreceptor terminals[14,15] and is known for its association with X-linked congenital stationary night blindness.[16] When compared to wild-type RIM1 (WT), R655H significantly increased the non-inactivating component of P/Q-type $Ca_v2.1$ currents (from 0.30 ± 0.04 (n = 6) to 0.43 ± 0.03 (n = 9); $p < 0.01$) (Fig. 1C). Inactivation parameters of L-type $Ca_v1.4$ currents were unaffected by R655H RIM1 (Fig. 1D) (see Table 1 for the estimated half-inactivation potential and the slope factor). In terms of activation properties, the voltage dependence of P/Q-type ($Ca_v2.1$) current activation was shifted toward negative potentials (see Table 1 for the voltages for half-maximal activation) and activation speed was increased by R655H expression (Fig. 2A). Furthermore, RIM1-mediated augmentation of $Ca_v2.1$ current density was significantly enhanced by R655H (Fig. 2B) (see Table 1 for current densities). In contrast to $Ca_v2.1$ currents, the RIM1-mediated hyperpolarizing shift of $Ca_v1.4$ activation was abolished by the mutation (Fig. 2C). The effects of R655H on activation speed (Fig. 2C) and current density were indistinguishable from those of WT RIM1 for $Ca_v1.4$ channels (Fig. 2D).

Here, we demonstrate that the mouse RIM1 mutant R655H, equivalent to the human CORD7 mutation, alters RIM1 function in regulating VDCC currents. For P/Q-type $Ca_v2.1$ VDCC, important in neurotransmitter release at central synapses, the CORD7 mutation accelerated activation, and enhanced the RIM1-mediated suppression of inactivation and augmentation of current density, likely leading to enhanced neurotransmitter release and synaptic transmission. In contrast, for L-type $Ca_v1.4$ VDCC, a predominent player in glutamate release from photoreceptor terminals, the CORD7 mutation abolished the RIM1-mediated hyperpolarization of current activation, likely resulting in impaired synaptic transmission at ribbon synapses of the visual system. The variable effects of this CORD7 mutation on different presynaptic VDCCs may underlie the two reported nervous system phenotypes, retinal dystrophy and enhanced cognitive abilities.

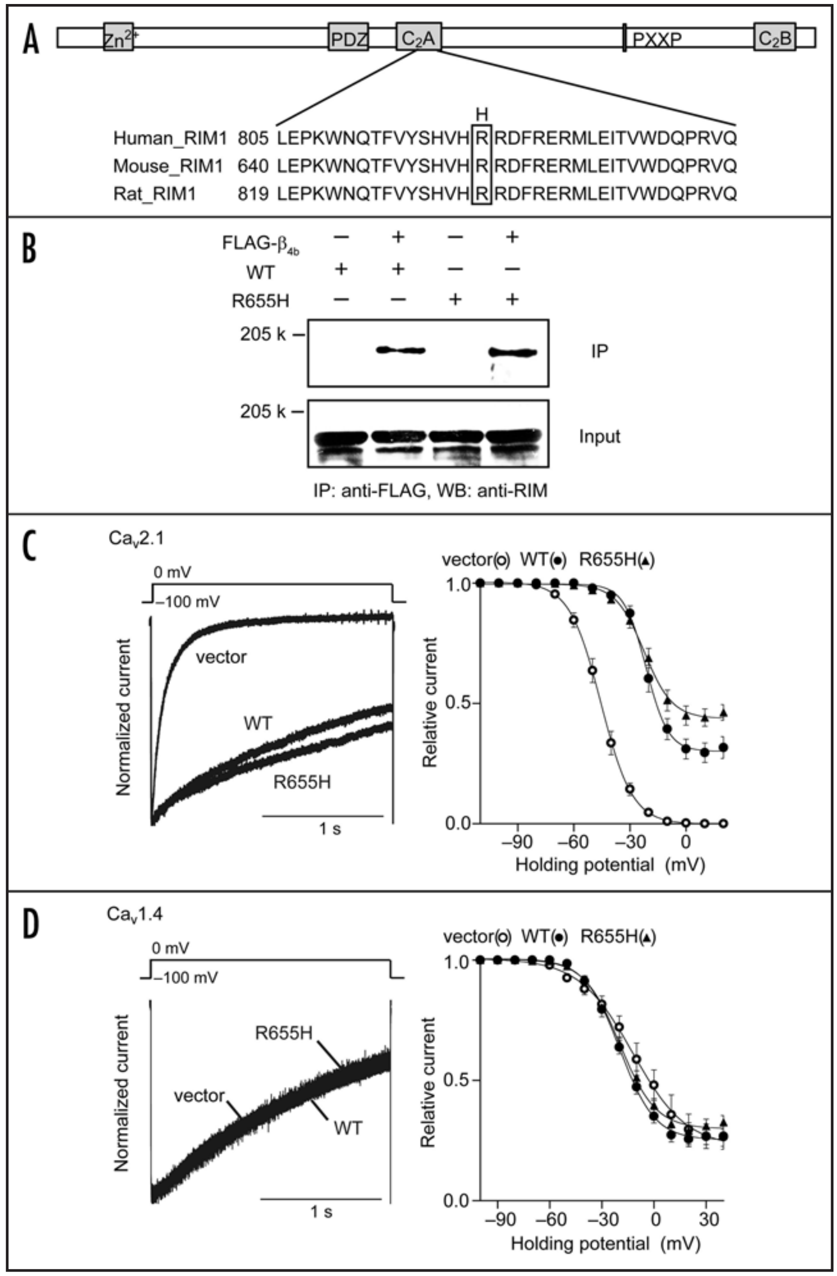

Figure 1. CORD7 mutation R655H affects regulation of $Ca_v2.1$ channel inactivation by RIM1 via β association. (A) Amino acid sequence alignment of C_2A domains of human, mouse and rat RIM1 (GenBank accession number NM_014989, NM_053270 and NM_052829, respectively). The position of the CORD7 substitution (H) is indicated. (B) Physical association of recombinant β_{4b} and R655H in HEK293 cells. The interaction is evaluated by immunoprecipitation (IP) with anti-FLAG antibody, followed by western blotting (WB) with anti-RIM antibody. Co-immunoprecipitation of wild-type RIM1 (WT) or R655H with FLAG-β_{4b}. (C) Effects of WT and R655H on the inactivation properties of P/Q-type $Ca_v2.1$ currents in BHK cells co-expressing α_2/δ and β_{4b}. Left panel, inactivation of P/Q-type $Ca_v2.1$ currents. The peak amplitudes are normalized for Ba^{2+} currents elicited by 2-s pulses to 0 mV from a holding potential (V_h) of -100 mV before and after expression of WT or R655H. Right panel, inactivation curves of P/Q-type $Ca_v2.1$ currents in BHK cells co-expressing α_2/δ and β_{4b}. The voltage dependence of inactivation, determined by measuring the amplitude of the peak currents evoked by 20-ms test pulses to 0 mV following 2-s prepulses to potentials from -100 to 20 mV with increments of 10 mV from a V_h of -100 mV, was fitted with the Boltzmann's equation. (D) Effects of WT and R655H on the inactivation properties of L-type $Ca_v1.4$ currents in BHK cells co-expressing α_2/δ and β_{4b}. Left panel, inactivation of L-type $Ca_v1.4$ currents. Right panel, inactivation curves of L-type $Ca_v1.4$ currents in BHK cells co-expressing α_2/δ and β_{4b}. The voltage dependence of inactivation is determined as in (C) above.

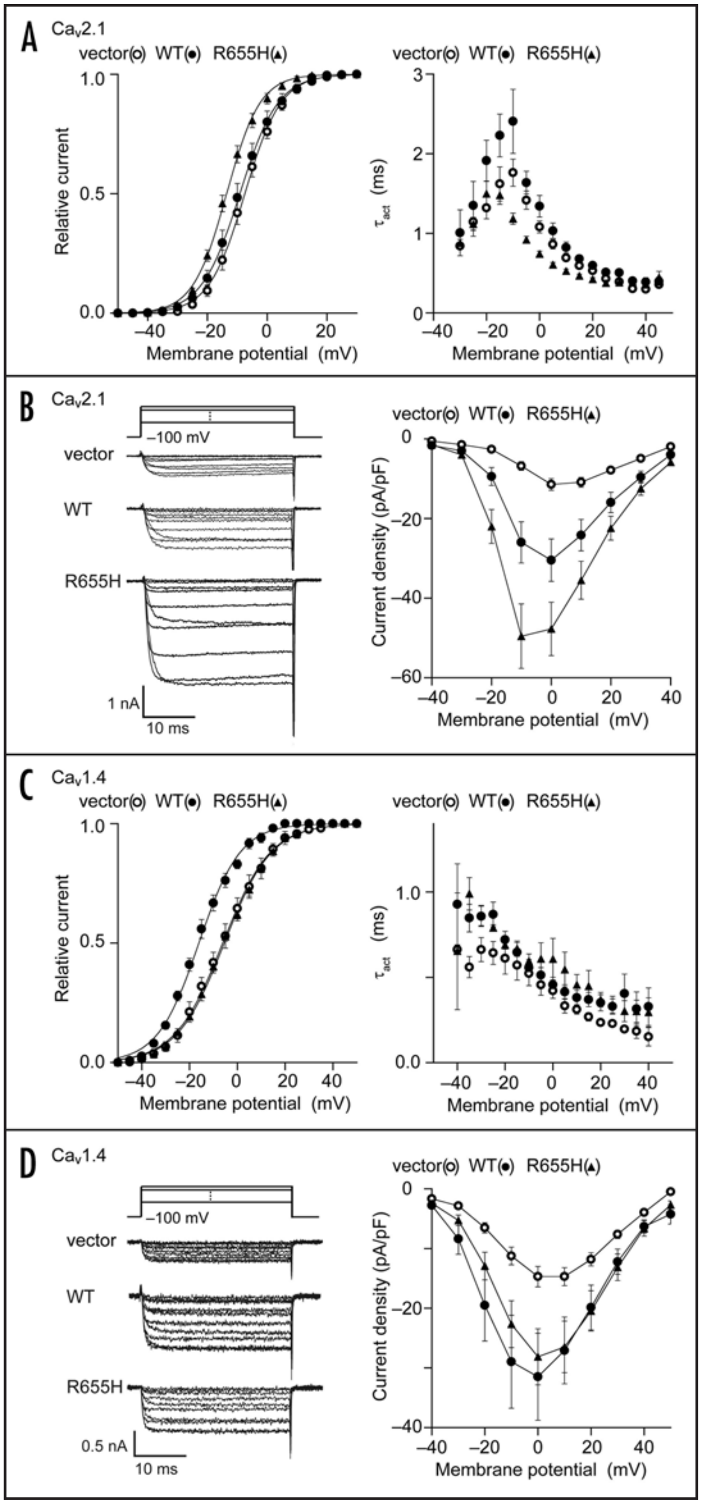

Figure 2. CORD7 mutation R655H affects regulation of $Ca_v2.1$ and $Ca_v1.4$ channel activation by RIM1 via β association. (A) Effects of WT and R655H on activation properties of $Ca_v2.1$ currents in BHK cells co-expressing α_2/δ and β_{4b}. Left pane, effects of WT and R655H on activation curves of $Ca_v2.1$ currents. Tail currents elicited by repolarization to -60 mV after 5-ms test pulse from -50 to 30 mV are used to determine activation curves. Right panel, effects on activation speed of $Ca_v2.1$ channels. Time constants are obtained by fitting the activation phase of currents elicited by 5-ms test pulse from -30 to 45 mV with a single exponential function. The differences between WT and R655H are significant at membrane potentials from -10 to 25 mV ($p < 0.001$, ANOVA, Fisher's test). (B) Effects of WT and R655H on $Ca_v2.1$ current amplitude. Left panel, representative traces for Ba^{2+} currents evoked by test pluses from -40 to 40 mV with 10-mV increments in BHK cells co-expressing α_2/δ and β_{4b}. Right panel, current density-voltage (*I–V*) relationships of $Ca_v2.1$. The V_h is -100 mV. (C) Effects of WT and R655H on activation properties of $Ca_v1.4$ currents in BHK cells co-expressing α_2/δ and β_{4b}. Left panel, effects of WT and R655H on activation curves of $Ca_v1.4$ currents. Right panel, effects on activation speed of $Ca_v1.4$ channels. (D) Effects of WT and R655H on $Ca_v1.4$ current amplitude. Left panel, representative traces for Ba^{2+} currents evoked by test pluses from -40 to 50 mV with 10-mV increments in BHK cells co-expressing α_2/δ and β_{4b}. Right panel, *I-V* relationships of $Ca_v1.4$. The V_h is -100 mV.

Acknowledgements

We thank E. Mori for expert experiments. This study was supported by research grants from the Ministry of Education, Culture, Sports, Science and Technology of Japan, the Japan Society for the Promotion of Science.

Reference

1. Wang Y, Okamoto M, Schmitz F, Hofmann K, Südhof TC. Rim is a putative Rab3 effector in regulating synaptic-vesicle fusion. Nature 1997; 388:593-8.
2. Wang Y, Sugita S, Südhof TC. The RIM/NIM family of neuronal C2 domain proteins. J Biol Chem 2000; 275:20033-44.
3. Betz A, Thakur P, Junge HJ, Ashery U, Rhee JS, Scheuss V, Rosenmund C, Rettig V, Brose N. Functional interaction of the active zone proteins Munc13-1 and RIM1 in synaptic vesicle priming. Neuron 2001; 30:183-96.
4. Ohtsuka T, Takao-Rikitsu E, Inoue E, Inoue M, Takeuchi M, Matsubara K, Deguchi-Tawarada M, Satoh K, Morimoto K, Nakanishi H, Takai Y. CAST: A novel protein of the cytomatrix at the active zone of synapses that forms a ternary complex with RIM1 and Munc13-1. J Cell Biol 2002; 158:577-90.
5. Schoch S, Castillo PE, Jo T, Mukherjee K, Geppert M, Wang Y, Schmitz F, Malenka RC, Südhof TC. RIM1α forms a protein scaffold for regulating neurotransmitter release at the active zone. Nature 2002; 415:321-6.
6. Coppola T, Magnin-Lüthi S, Perret-Menoud V, Gattesco S, Schiavo G, Regazzi R. Direct interaction of the Rab3 effector RIM with Ca^{2+} channels, SNAP-25, and Synaptotagmin. J Biol Chem 2001; 276:32756-62.
7. Castillo PE, Schoch S, Schmitz F, Südhof TC, Malenka RC. RIM1α is required for presynaptic long-term potentiation. Nature 2002; 415:327-30.
8. Schoch S, Mittelstaedt T, Kaeser PS, Padgett D, Feldmann N, Chevaleyre V, Castillo PE, Hammer RH, Han W, Schmitz F, Lin W, Südhof TC. Redundant functions of RIM1α and RIM2α in Ca^{2+}-triggered neurotransmitter release. EMBO J 2006; 25:5852-63.
9. Johnson S, Halford S, Morris AG, Patel RJ, Wilkie SE, Hardcastle AJ, Moore AT, Zhang K, Hunt DM. Genomic organization and alternative splicing of human *RIM1*, a gene implicated in autosomal dominant cone-rod dystrophy *(*CORD7*)*. Genomics 2003; 81:304-14.
10. Kelsell RE, Gregory-Evans K, Gregory-Evans CY, Holder GE, Jay MR, Weber BHF, Moore AT, Biro AC, Hunt DM. Localization of a Gene (*CORD7*) for a dominant cone-rod dystrophy to chromosome 6q. Am J Hum Genet 1998; 63:274-9.
11. Sisodiya S, Thompson P, Need A, Harris S, Weale M, Wilkie S, Michaelides M, Free S, Walley N, Gumb C, Gerrelli D, Ruddle P, Whalley L, Starr J, Hunt D, David G, Deary I, Moore A. Genetic enhancement of cognition in a kindred with cone-rod dystrophy due to *RIMS1* mutation. J Med Genet 2007; 44:373-80.
12. Kiyonaka S, Wakamori M, Miki T, Uriu Y, Nonaka M, Bito H, Beedle AM, Mori E, Hara Y, De Waard M, Kanagawa M, Itakura M, Takahashi M, Campbell KP, Mori Y. RIM1 confers sustained activity and neurotransmitter vesicle anchoring to presynaptic Ca^{2+} channels. Nat Neurosci 2007; 10:691-701.
13. Tsien RW, Ellinor PT, Horne WA. Molecular diversity of voltage-dependent Ca^{2+} channels. Trens Pharmacol Sci 1991; 12:349-54.
14. Koschak A, Reimer D, Walter D, Hoda JC, Heinzle T, Grabner M, Striessnig J. $Ca_v1.4\alpha1$ subunits can form slowly inactivating dihydropyridine-sensitive L-type Ca^{2+} channels lacking Ca^{2+}-dependent inactivation. J Neurosci 2003; 23:6041-9.
15. McRory JE, Hamid J, Doering CJ, Garcia E, Parker R, Hamming K, Chen L, Hildebrand M, Beedle AM, Feldcamp L, Zamponi GW, Snutch TP. The *CACNA1F* gene encodes an L-type calcium channel with unique biophysical properties and tissue distribution. J Neurosci 2004; 24:1707-18.
16. Bech-Hansen NT, Naylor MJ, Maybaum TA, Pearce WG, Koop B, Fishman GA, Mets M, Musarella MA, Boycott KM. Loss-of-function mutations in a calcium-channel α_1-subunit gene in *Xp11*.23 cause incomplete X-linked congenital stationary night blindness. Nat Genet 1998; 19:264-7.

Table 1 **Effects of WT and R655H on current density, activation and inactivation of $Ca_v2.1$, or $Ca_v1.4$ channel[1)2)]**

		Current Density	Activation Parameters[4]		Inactivation Parameters[5]		
		(pA / pF)[3]	$V_{0.5}$ (mV)	k (mV)	a	$V_{0.5}$ (mV)	k (mV)
$Ca_v2.1$	vector	-11.4 ± 1.5 (14)	-7.2 ± 1.2 (10)	4.5 ± 1.3 (10)	1.00 ± 0.00 (12)	-45.9 ± 1.8 (12)	-7.5 ± 0.3 (12)
	WT	-30.5 ± 5.3 (16)*	-9.1 ± 1.6 (13)	5.6 ± 0.2 (13)	0.70 ± 0.04 (6)***	-21.3 ± 1.2 (6)***	-5.6 ± 0.7 (6)
	R655H	-47.7 ± 6.7 (24)***#	-13.3 ± 0.9 (24)**#	5.1 ± 0.2 (24)	0.57 ± 0.03 (9)***#	-22.0 ± 1.2 (9)***	-8.0 ± 1.0 (9)#
$Ca_v1.4$	vector	-14.7 ± 1.7 (23)	-6.1 ± 1.8 (6)	9.7 ± 0.8 (6)	0.79 ± 0.06 (5)	-10.5 ± 3.4 (5)	-15.1 ± 1.0 (5)
	WT	-31.5 ± 7.3 (19)*	-16.2 ± 1.0 (8)***	8.3 ± 0.5 (8)	0.75 ± 0.03 (7)	-19.5 ± 1.8 (7)*	-9.7 ± 0.3 (7)***
	R655H	-28.1 ± 4.7 (23)*	-5.4 ± 0.9 (6)##	9.9 ± 0.6 (6)	0.73 ± 0.02 (10)	-18.0 ± 1.6 (10)*	-10.8 ± 0.7 (10)***

[1]*$p < 0.05$, **$p < 0.01$, ***$p < 0.001$ versus vector (ANOVA, Fisher's test). [2]#$p < 0.05$, #$p < 0.01$, ##$p < 0.001$ versus WT (ANOVA, Fisher's test). [3]Amplitudes of Ba^{2+} currents evoked by depolarizing pulse to 0 mV from a V_h of -100 mV are divided by capacitance. [4]$V_{0.5}$ is the half-maximal activation voltage, and k is the slope factor. [5]a is the rate of inactivating component, $V_{0.5}$ is the half-inactivation potential and k is the slope factor.